GSA Data Repository 2016309

Tectonic and climate controls on Neogene environmental change in the Zhada Basin, southwestern Tibetan Plateau

Saylor et al.

METHODS

Prior to stable isotope analysis, sediment samples were crushed and treated with 30% H_2O_2 to remove organic material. Stable isotopes of oxygen and carbon in bulk carbonate samples (expressed as $\delta^{18}O_c$ and $\delta^{13}C_c$ in units ‰, respectively, and referenced to Vienna Pee Dee Belemnite (VPDB) were measured using a Finnigan MAT 252 gas-ratio mass spectrometer at the University of Texas at Austin. Sample ages were determined by linear interpolation between paleomagnetic ties of the preferred magnetostratigraphic correlation of Saylor et al. (2009).

For grain size analysis, samples were disaggregated by soaking in an aqueous solution of hexametaphosphate for at least 3 days. They were subsequently placed in an ultrasonic bath for four hours to deflocculate clays. Samples were removed from the ultrasonic bath and immediately analyzed in a Cilas 1190 laser-diffraction particle size analyzer at the University of Houston which analyzes grain sizes between 4 and 2,500 µm. All samples were analyzed in triplicate to ensure that deflocculation was successful.

DISCUSSION

Relationship between onset of lacustrine conditions and late Miocene ISM intensification

The emergence of paleo-Lake Zhada at ~ 6.0 Ma post-dates the evidence for the onset of regional intensification of the monsoon system (Barry et al., 1985; Kroon et al., 1991; Prell and Kutzbach, 1992; Quade et al., 1995) suggesting that there is not a direct causal correlation between late Miocene intensification of the monsoon and basin flooding. However, following establishment of paleo-Lake Zhada, expansion and contraction of the lake is recorded by high-frequency variations in mean grain size, $\delta^{18}O_c$ and $\delta^{13}C_c$ values, and rapid lithofacies changes in interval B. These high-frequency variations reflect changes in lake volume attributable to changing precipitation/evaporation due to the strengthening and weakening of ISM precipitation (Kempf et al., 2009; Saylor et al., 2010).

Transition to Interval C

An alternative interpretation for the increase in depositional energy and decrease in $\delta^{18}O_c$ and $\delta^{13}C_c$ values seen at the transition from B to C in the SZ stratigraphic section is reestablishment of a through-going drainage following overtopping of the basin sill or the onset of incision. However, we discount this possibility because it does not explain either the persistent lacustrine lithofacies observed at the SEZ location or the intermittent lacustrine conditions observed at the SZ location. It is also inconsistent with the increase in $\delta^{18}O_c$ values observed in interval C at the SEZ location. Similarly, an increase in precipitation/evaporation would lead to increased lake size, shoreline retrogradation, and decreasing grain size rather than the observed progradation and grain size coarsening (Fig. 2).

We interpret the increased variability in grain size and δ_c values in interval C as indicating increased variability of influx to the paleo-Lake Zhada. Interval C shows a greater variability in both grain size and $\delta^{18}O_c$ values than interval B at the SZ location and in $\delta^{18}O_c$ values SEZ locations. Interval C at the SZ location also has greater average grain size and greater grain size variability than either interval A or B. Although the variation in $\delta^{18}O_c$ values in interval A is as great as that in interval C, we attribute it to a different mechanism. $\delta^{18}O_c$ values in the overfilled, fluvially dominated interval A reflect evaporative enrichment in overbank depositional settings due to non-systematic river migration. Hence variation in $\delta^{18}O_c$ values in this depositional system requires no significant change in discharge. However, in the under- or balance filled lacustrine intervals B and C, freshening lacustrine water or rapid shoreline retrogradation requires large variations in fluvial discharge.

Relationship between lake shrinking and decreasing $\delta^{18}O$ values

We discount an increase in precipitation/evaporation as an explanation for the decrease in mean δ_c values and increase in grain sizes observed in interval C for the following reasons. An increase in precipitation/evaporation could potentially increase the discharge of rivers flowing into Zhada Basin, bringing coarser material into the basin. However, following observations in the Holocene, an increase in precipitation/evaporation would be expected to increase lake size (Hudson and Quade, 2013). The decrease in transport energy as flowing water enters stagnant lake waters results in rapid deposition of coarse sand–boulder material at the lake margins. Hence, an increase in lake area due to increased precipitation/evaporation would not be expected to result in an extreme increase in grain size (up to boulder conglomerate) as is observed in interval C. However, the high variability in $\delta^{18}O_c$ values in interval C is consistent with high frequency (< 0.5 Myr) fluctuations in precipitation/evaporation superimposed on a long-term record of increased aridity. High frequency, high amplitude variability of precipitation amount would result in rapid shoreline progradation and retrogradation, and intermittent freshening of the water in the basin.

We attribute the high correlation coefficients despite extremely negative $\delta^{18}O_c$ and $\delta^{13}C_c$ values in stratigraphic section SZ to mixing between isotopically lighter inflowing water and isotopically heavier lacustrine water (Platt, 1989; Arenas et al., 1997; Tanner, 2000). Correlations are a function of mixing or evolution between two end members and so high correlations are consistent with mixing between fluvial or palustrine and lacustrine isotopic compositions.

Although we cannot rule out a decrease in lake size due to infilling of the lake basin in the absence of any climate change, this is not our favored scenario because independent evidence points to local aridification after the early Pliocene. First, a coeval positive shift in $\delta^{18}O_c$ values and persistent lacustrine deposition in the SEZ stratigraphic section argue against a local progradation in the absence of climate change. Second, $\delta^{18}O$ values from mammal megafauna tooth enamel are more negative before 3.5 Ma than they are now (Wang et al., 2013). $\delta^{18}O$ values of bioapatite from large mammals are strongly correlated with local precipitation $\delta^{18}O$ values (Kohn and Cerling, 2002; Wang et al., 2008). Wang et al. (2013) conclude that precipitation $\delta^{18}O$ values were more negative in the early Pliocene than in the modern. They further conclude that because precipitation $\delta^{18}O$ values are strongly controlled by precipitation amounts in the modern ISM system, more negative early Pliocene precipitation $\delta^{18}O$ values point to wetter conditions. Third, decreasing precipitation/evaporation is consistent with the conclusions of Zhu et al. (2007) that the Zhada Basin experienced increased aridity at about the 500 m level in the stratigraphic section (~3.5 Ma based on the age model of Saylor et al. (2009)). Finally, Kempf et al. (2009) found high salinity tolerant ostracods in intervals B and C, whereas they were absent in interval A. While their absence from the record in interval A may be accidental, their presence in interval C points to evaporative conditions and standing water, consistent with the interpretation of a persistent but smaller lake. All of this evidence points to local aridification in the Zhada Basin in the middle Pliocene. Future research is needed to verify the results of this investigation on a regional basis.

Potential mechanisms

General circulation models incorporating surface uplift in the northern or eastern Tibetan Plateau predict increased East Asian Monsoon (EAM) strength but decreased ISM strength (An et al., 2001; Tang et al., 2013), both of which have been noted (Nie et al., 2014). However, major deformation and tectonic reorganization in the northeastern Tibetan Plateau was accomplished by the middle–late Miocene (Yuan et al., 2013).

Increased aridity at 3.5 ± 0.1 Ma in the Zhada Basin suggests a limited effect of late Pliocene Pacific cooling and increase in zonal Pacific SST gradients on ISM circulation over the southern Tibetan Plateau (Fig. 3). Nie et al. (2014) linked cooling and freshening in the North Pacific in response to cooling and freshening in the eastern tropical Pacific to increasing mean annual precipitation on the Chinese Loess Plateau and an increase in the strength of the East Asian Monsoon (EAM) (Haug et al., 2001). Similarly, an increased zonal SST gradient starting at 3–4 Ma in the Pacific (Zhang et al., 2014) is linked to an increase in EAM strength. However, both cooling of the eastern tropical Pacific, and an increase in zonal sea surface temperature gradients should be correlated with increased precipitation on the southern Tibetan Plateau, rather than the observed increase in aridity. An increase in meridional eastern Pacific SSTs may account for the observed middle Pliocene decrease in ISM strength, but also predicts a decrease in EAM strength, contrary to observations (Brierley et al., 2009; Nie et al., 2014).

Table DR1: Carbonate bulk sediment stable isotope compositions, and grain size data for the three stratigraphic sections.

Table DR2: Means, standard deviations, and ANOVA statistics of mean grain size and $\delta^{18}O_c$ and $\delta^{13}C_c$ values from Zhada Basin.

Table DR3. Lithofacies codes and interpretation

FIGURES

Figure DR1. Sequence stratigraphic correlation of the measured sections in the Zhada Basin. The transition from interval A to B occurs at maximum flooding surface 1 (MFS1). The transition from B to C occurs in the highstand prior to sequence boundary 3 (SB3). Abbreviations: SB: Sequence boundary, MFS: Maximum flooding surface, TS: Transgressive surface, C: Claystone, S: Siltstone, SS: Sandstone, Cgm: Conglomerate. See Table DR3 for lithofacies descriptions.

Figure DR2. $\delta^{18}O_c$ and $\delta^{13}C_c$ cross-plots and correlation coefficients for intervals A, B, and C from the SZ stratigraphic section.

Figure DR3. $\delta^{18}O_c$ and $\delta^{13}C_c$ cross-plots and correlation coefficients for intervals A and B from the EZ stratigraphic section.

Figure DR4. $\delta^{18}O_c$ and $\delta^{13}C_c$ cross-plots and correlation coefficients for intervals A, B, and C from the SEZ stratigraphic section. Outlying data point has a $\delta^{13}C_c$ value that is more than 3σ from the mean of the remainder of the population. The preferred correlation coefficient (black linear fit and text) excludes the outlier, while the light grey linear fit and correlation coefficient include the outlier.

Works Cited

An, Z.-s., Kutzbach, J. E., Prell, W. L., and Porter, S. C., 2001, Evolution of Asian monsoons and phased uplift of the Himalaya-Tibetan plateau since late Miocene times: Nature, v. 311, p. 62-66.

Arenas, C., Casanova, J., and Pardo, G., 1997, Stable-isotope characterization of the Miocene lacustrine systems of Los Monegros (Ebro Basin, Spain): palaeogeographic and palaeoclimatic implications: Palaeogeography, Palaeoclimatology, Palaeoecology, v. 128, no. 1–4, p. 133-155.

Barry, J. C., Johnson, N. M., Raza, S. M., and Jacobs, L. L., 1985, Neogene mammalian faunal change in southern Asia: Correlations with climatic, tectonic, and eustatic events: Geology, v. 13, no. 9, p. 637-640.

Brierley, C. M., Fedorov, A. V., Liu, Z., Herbert, T. D., Lawrence, K. T., and LaRiviere, J. P., 2009, Greatly Expanded Tropical Warm Pool and Weakened Hadley Circulation in the Early Pliocene: Science, v. 323, no. 5922, p. 1714-1718.

Haug, G. H., Tiedemann, R., Zahn, R., and Ravelo, A. C., 2001, Role of Panama uplift on oceanic freshwater balance: Geology, v. 29, no. 3, p. 207-210.

Hudson, A. M., and Quade, J., 2013, Long-term east-west asymmetry in monsoon rainfall on the Tibetan Plateau: Geology, v. 41, no. 3, p. 351-354.

Kempf, O., Blisniuk, P. M., Wang, S., Fang, X., Wrozyna, C., and Schwalb, A., 2009, Sedimentology, sedimentary petrology, and paleoecology of the monsoon-driven, fluviolacustrine Zhada Basin, SW-Tibet: Sedimentary Geology, v. 222, p. 27-41.

Kohn, M. J., and Cerling, T. E., 2002, Stable isotope compositions of biological apatite, *in* Kohn, M., Rakovan, J., and Hughes, J., eds., Phosphates â€“ Geochemical, Geobiological, and Materials Importance, Volume 48: Washington, D.C., Mineralogical Society of America, p. 455-488.

Kroon, D., Steens, T., and Troelstra, S., 1991, Onset of monsoonal related upwelling in the western Arabian Sea as revealed by planktonic foraminifers, Procedings of the Ocean Drilling Program: Scientific Results.

Nie, J., Stevens, T., Song, Y., King, J. W., Zhang, R., Ji, S., Gong, L., and Cares, D., 2014, Pacific freshening drives Pliocene cooling and Asian monsoon intensification: Scientific Reports, v. 4, p. 5474.

Platt, N. H., 1989, Lacustrine carbonates and pedogenesis - Sedimentology and origin of palustrine deposits from the Early Cretaceous Rupelo Formation, W Cameros Basin, N Spain: Sedimentology, v. 36, no. 4, p. 665-684.

Prell, W., and Kutzbach, J., 1992, Sensitivity of the Indian monsoon to forcing parameters and implications for its evolution: Nature, v. 360, no. 6405, p. 647-652.

Quade, J., Cater, J., Ojha, T., Adam, J., and Harrison, T., 1995, Late Miocene environmental change and in Nepal and the northern Indian subcontinent; stable isotopic evidence from paleosols: Geological Society of America Bulletin, v. 107, no. 12, p. 1381-1397.

Saylor, J. E., DeCelles, P. G., and Quade, J., 2010, Climate-driven environmental change in the Zhada basin, southwestern Tibetan Plateau: Geosphere, v. 6, no. 2, p. 74-92.

Saylor, J. E., Quade, J., Dettman, D. L., DeCelles, P. G., Kapp, P. A., and Ding, L., 2009, The late Miocene through present paleoelevation history of southwestern Tibet: American Journal of Science, v. 309, no. 1, p. 1-42.

Tang, H., Micheels, A., Eronen, J. T., Ahrens, B., and Fortelius, M., 2013, Asynchronous responses of East Asian and Indian summer monsoons to mountain uplift shown by regional climate modelling experiments: Climate Dynamics, v. 40, no. 5-6, p. 1531-1549.

Tanner, L. H., 2000, Palustrine-Lacustrine and Alluvial Facies of the (Norian) Owl Rock Formation (Chinle Group), Four Corners Region, Southwestern U.S.A: Implications for Late Triassic Paleoclimate: Journal of Sedimentary Research, v. 70, no. 6, p. 1280-1289.

Wang, Y., Kromhout, E., Zhang, C., Xu, Y., Parker, W., Deng, T., and Qiu, Z., 2008, Stable isotopic variations in modern herbivore tooth enamel, plants and water on the Tibetan Plateau: Implications for paleoclimate and paleoelevation reconstructions: Palaeogeography, Palaeoclimatology, Palaeoecology, v. 260, p. 359-374.

Wang, Y., Xu, Y. F., Khawaja, S., Passey, B. H., Zhang, C., Wang, X., Qiang, L., Tseng, Z. J., Takeuchi, G. T., Deng, T., and Xie, G. P., 2013, Diet and environment of a mid-Pliocene fauna from southwestern Himalaya: Paleo-elevation implications: Earth and Planetary Science Letters.

Yuan, D.-Y., Ge, W.-P., Chen, Z.-W., Li, C.-Y., Wang, Z.-C., Zhang, H.-P., Zhang, P.-Z., Zheng, D.-W., Zheng, W.-J., Craddock, W. H., Dayem, K. E., Duvall, A. R., Hough, B. G., Lease, R. O., Champagnac, J.-D., Burbank, D. W., Clark, M. K., Farley, K. A., Garzione, C. N., Kirby, E., Molnar, P., and Roe, G. H., 2013, The growth of northeastern Tibet and its relevance to large-scale continental geodynamics: A review of recent studies: Tectonics, v. 32, no. 5, p. 2013TC003348.

Zhang, Y. G., Pagani, M., and Liu, Z., 2014, A 12-Million-Year Temperature History of the Tropical Pacific Ocean: Science, v. 344, no. 6179, p. 84-87.

Zhu, D., Meng, X., Shoa, Z., Yang, C., Han, J., Yu, J., Meng, Q., and Lu, R., 2007, Evolution of the paleovegatation, paleoenvironment and paleoclimate during Pliocene - early Pleistocene in Zhada Basin, Ali, Tibet: Acta Geologica Sinica, v. 81, p. 295-306.

Table DR1: Carbonate bulk sediment stable isotope compositions, and grain size data for the three stratigraphic sections.

						Grain size parameters							
SAMPLE	Stratigraphic Level (m)	Age (Ma)	MEAN (µm)	MODE 1 (µm)	MODE 2 (µ	MODE 3 (µ	D10 (µm)	MEDIAN o	D90 (µm)	(D75 / D25)	(D75 - D25) (µm)	$\delta^{13}C$ (‰ PDB)	$\delta^{18}O$ (‰ PDB)
SZ Stratigraphic Section													
LC20	20	Below lowest tie point	817.0	97.5	73.0	39.0	18.3	629.4	2206.1	16.7	1518.5	0.5	-7.1
LC22.5	22.5	Below lowest tie point	542.6	54.5	39.0	19.5	14.9	152.1	1963.8	20.0	959.8	-2.5	-15.5
LC24.5	24.5	Below lowest tie point	698.3	73.0	39.0	54.5	14.9	247.3	2130.0	23.0	1363.7	1.0	-9.5
LC26.25	26.25	Below lowest tie point	678.7	39.0	54.5	19.5	15.7	229.2	2113.9	22.8	1324.2	1.1	-15.2
LC28.5	28.5	Below lowest tie point	830.0	97.5	73.0	54.5	20.7	661.3	2212.4	15.7	1527.2	1.4	-10.3
LC30.5	30.5	Below lowest tie point	691.2	97.5	73.0	54.5	23.6	247.0	2113.1	14.3	1286.4	0.7	-11.6
LC32.5	32.5	Below lowest tie point	624.3	39.0	54.5	19.5	14.5	188.6	2063.8	24.0	1207.4	0.9	-9.5
LC34.25	34.25	Below lowest tie point	612.6	54.5	39.0	19.5	17.4	186.7	2046.1	18.2	1149.5	0.6	-7.6
LC36.5	36.5	Below lowest tie point	738.1	97.5	73.0	54.5	22.2	353.9	2156.1	17.9	1408.0	1.6	-7.7
LC38.5	38.5	Below lowest tie point	695.3	73.0	54.5	39.0	15.9	247.1	2123.9	18.5	1334.2	-3.9	-18.2
LC42.5	42.5	8.99	615.0	54.5	39.0	19.5	16.3	189.9	2048.8	19.3	1159.6	1.0	-12.3
LC44.5	44.5	8.97	568.5	39.0	54.5	19.5	13.5	159.1	2003.1	25.0	1063.3	-5.2	-17.7
LC52.25	52.25	8.91	583.8	54.5	39.0	19.5	13.9	175.6	2015.4	21.0	1083.9	1.0	-10.0
LC57.5	57.5	8.86	651.6	39.0	54.5	19.5	14.8	207.2	2088.2	22.5	1261.8	-0.1	-13.9
LC59.25	59.25	8.84	614.8	54.5	39.0	19.5	16.2	191.1	2048.1	19.4	1158.2	0.1	-13.1
LC61.25	61.25	8.83	609.1	54.5	39.0	19.5	14.3	182.6	2046.7	22.8	1164.3	0.5	-10.0
LC63.25	63.25	8.81	597.8	39.0	54.5	19.5	12.7	176.3	2036.5	25.6	1145.7	0.1	-13.3
LC65.25	65.25	8.79	571.8	39.0	54.5	19.5	14.9	164.7	2003.9	21.9	1059.0	-1.4	-16.5
LC67.25	67.25	8.77	569.8	39.0	54.5	19.5	15.6	161.7	2001.9	21.7	1053.9	0.4	-12.2
LC69.5	69.5	8.75	562.4	39.0	54.5	19.5	12.5	149.5	1892.2	23.4	938.3	0.4	-12.7
LC71.25	71.25	8.74	543.5	54.5	39.0	19.5	13.6	152.4	1966.2	21.6	969.3	0.8	-12.5
LC73.25	73.25	8.72	552.1	39.0	54.5	19.5	13.5	151.7	1981.0	23.9	1008.4	0.4	-10.7
0.1SZ17.5	98.25	8.13	511.4	39.0	54.5	19.5	15.4	140.5	1921.7	22.3	864.3	-0.2	-12.3
0.1SZ19.5	100.25	8.08	661.0	39.0	54.5	19.5	18.0	211.0	2095.3	18.9	1267.1	0.0	-12.7
0.1SZ21.5	102.25	8.05	491.6	39.0	54.5	19.5	11.3	128.6	1894.4	23.2	798.9	-4.7	-16.3
0.1SZ23.5	104.25	8.03	507.4	39.0	54.5	19.5	15.3	138.2	1916.1	22.6	851.3	-1.9	-13.6
0.1SZ25.0	105.75	8.01	520.9	39.0	54.5	19.5	15.5	143.8	1934.5	20.7	891.3	-1.8	-14.3
0.1SZ27.0	107.75	7.99	576.8	39.0	54.5	19.5	14.0	162.6	2012.9	24.8	1086.3	-0.3	-13.4
0.1SZ29.0	109.75	7.96	576.6	54.5	39.0	19.5	17.5	170.3	2005.2	18.8	1053.8	-4.4	-18.6
0.1SZ31.0	111.75	7.94	601.9	39.0	54.5	19.5	17.5	182.0	2035.3	20.3	1130.6	-1.0	-15.2
0.1SZ33.0	113.75	7.91	526.5	39.0	54.5	19.5	16.9	145.5	1941.5	19.8	906.0	-5.5	-14.4
0.1SZ35.0	115.75	7.89	515.7	39.0	54.5	19.5	15.6	142.0	1927.4	21.6	876.5	-2.1	-11.7
0.1SZ37.0	117.75	7.86	528.8	39.0	54.5	19.5	16.9	146.3	1944.5	19.6	912.6	-0.9	-13.2
0.1SZ38.5	119.25	7.85	590.2	39.0	54.5	19.5	16.7	174.2	2024.1	21.5	1106.2	-4.1	-17.1
0.1SZ39.0	119.75	7.84	657.6	39.0	54.5	19.5	18.0	206.7	2093.1	19.5	1263.9	-0.1	-13.1
0.1SZ41.0	121.75	7.82	519.7	54.5	39.0	19.5	15.1	143.4	1933.2	21.3	889.3	-3.5	-14.1
0.1SZ45.0	125.75	7.77	688.4	97.5	73.0	54.5	22.3	244.6	2115.3	16.8	1305.8	-0.8	-23.1
0.1SZ47.0	127.75	7.74	626.3	54.5	39.0	19.5	18.1	191.3	2061.7	19.5	1190.3	1.0	-13.6
0.1SZ49.0	129.75	7.72	653.8	73.0	54.5	39.0	19.1	205.8	2088.1	18.4	1248.7	0.9	-11.6
0.1SZ51.0	131.75	7.69	524.1	39.0	54.5	19.5	17.2	144.7	1938.3	20.1	898.9	0.5	-12.0
0.1SZ52	132.75	7.68	541.2	73.0	54.5	39.0	18.2	150.3	1960.0	18.9	948.6	-4.1	-15.9
0.1SZ57.0	137.75	7.62	512.1	39.0	54.5	19.5	15.6	140.7	1922.6	22.1	866.2	-2.4	-14.3
0.1SZ59.0	139.75	7.59	530.1	39.0	54.5	19.5	16.8	146.7	1946.3	19.5	916.7	-2.3	-15.1
0.1SZ61.0	141.75	7.57	530.9	54.5	39.0	19.5	15.4	147.2	1948.2	20.5	923.6	-3.1	-12.3
0.1SZ63.0	143.75	7.55	545.9	54.5	39.0	19.5	18.1	153.3	1966.1	18.8	962.0	-0.3	-13.0
0.1SZ65.0	145.75	7.52	505.6	39.0	54.5	19.5	13.6	137.2	1914.2	22.9	847.0	-0.1	-13.4

0.1SZ66.5	147.25	7.50	496.6	39.0	54.5	19.5	14.5	150.3	1963.3	22.6	964.7	-0.4	-14.0
0.1SZ68.5	149.25	7.48	737.8									0.6	-12.4
0.2SZ0.0	150.7	7.46	517.8	39.0	54.5	19.5	13.8	143.0	1931.5	23.3	889.0	-0.1	-13.8
0.1SZ70.5	151.25	7.45	812.5	97.5	73.0	54.5	29.3	603.0	2200.6	14.7	1492.4	-0.9	-13.7
0.2SZ2.0	152.7	7.44	854.9	97.5	73.0	39.0	22.2	718.4	2223.5	13.0	1531.4	0.7	-13.8
0.2SZ4.0	154.7	7.41	610.6	97.5	73.0	54.5	24.7	189.2	2037.9	15.0	1116.6	-0.2	-15.2
0.2SZ6.0	156.7	7.39	654.5	97.5	73.0	54.5	18.9	212.2	2085.1	16.9	1235.1	0.7	-13.7
0.2SZ8.0	158.7	7.36	557.7	54.5	39.0	19.5	18.6	160.4	1980.4	18.1	992.9	0.6	-14.6
0.2SZ10.0	160.7	7.34	628.6	73.0	39.0	54.5	19.5	194.6	2062.6	18.7	1189.9	-0.3	-12.1
0.2SZ12	162.7	7.31	507.0	39.0	54.5	19.5	13.9	138.2	1916.2	22.9	852.0	-0.8	-12.7
0.2SZ14.0	164.7	7.29	675.2	39.0	54.5	19.5	17.9	224.7	2109.2	19.8	1303.4	1.6	-11.0
0.2SZ16.0	166.7	7.27	567.5	73.0	54.5	39.0	20.3	166.0	1992.2	17.5	1018.5	-0.6	-13.9
0.2SZ20.0	170.7	7.22	524.4	54.5	39.0	19.5	15.1	145.0	1939.4	20.6	902.5	-4.0	-15.1
0.2SZ22.0	172.7	7.19	505.9	39.0	54.5	19.5	14.7	137.2	1914.3	22.6	846.7	-2.1	-13.9
0.2SZ24.0	174.7	7.17	524.9	39.0	54.5	19.5	15.0	145.2	1940.4	21.3	906.5	-2.3	-13.4
0.2SZ26.0	176.7	7.14	518.9	39.0	54.5	19.5	15.9	143.1	1931.8	21.2	885.9	-0.3	-12.3
0.2SZ30.0	180.7	7.09	562.6	39.0	54.5	19.5	16.1	163.4	1989.8	20.6	1022.0	0.7	-10.8
0.2SZ32.0	182.7	7.07	612.4	39.0	54.5	19.5	16.2	181.2	2051.2	23.4	1176.4	0.2	-12.7
0.3SZ2	199	6.57	631.2	97.5	73.0	54.5	18.8	197.9	2062.7	16.6	1181.4	0.2	-12.1
0.3SZ4	201	6.51	536.6	39.0	54.5	19.5	15.3	149.2	1956.1	20.8	943.8	-0.2	-11.4
0.3SZ6	203	6.45	603.8	97.5	73.0	54.5	20.7	185.4	2032.4	15.8	1106.9	-1.7	-12.8
0.3SZ8	205	6.38	714.4	97.5	73.0	39.0	18.9	272.5	2139.4	18.9	1372.3	1.2	-11.7
0.3SZ14	211	6.25	518.1	39.0	54.5	19.5	15.5	142.8	1930.7	21.2	883.3	-0.4	-11.2
0.3SZ18	215	6.21	554.9	54.5	39.0	19.5	18.4	158.8	1977.3	18.7	987.4	-0.6	-11.5
0.3SZ20	217	6.19	569.8	73.0	54.5	39.0	18.5	167.4	1994.8	16.4	1020.5	0.0	-13.2
0.3SZ24	221	6.15	664.9	97.5	73.0	54.5	25.7	219.2	2093.8	15.9	1250.3	0.7	-10.5
0.3SZ26	223	6.11	635.2	97.5	73.0	54.5	31.8	200.6	2062.5	14.9	1172.1	0.5	-11.5
0.3SZ28	225	6.00	557.5	73.0	54.5	39.0	18.8	160.4	1980.4	18.6	994.5	-0.6	-12.8
0.3SZ30	227	5.89	480.0	39.0	19.5	54.5	11.7	122.8	1876.2	25.6	760.3	1.3	-9.7
0.3SZ32	229	5.84	482.4	39.0	54.5	19.5	11.6	125.1	1880.1	25.0	769.1	1.2	-8.7
0.3SZ34	231	5.78	554.7	39.0	54.5	19.5	16.1	158.8	1980.1	20.8	999.5	0.9	-9.4
0.3SZ36	233	5.73	649.4	97.5	73.0	54.5	35.9	208.2	2073.4	13.4	1188.5	0.1	-11.1
0.3SZ38	235	5.67	457.3	39.0	19.5	54.5	8.8	106.0	1839.5	31.8	678.3	1.3	-10.0
0.3SZ40	237	5.62	455.2	39.0	19.5	54.5	8.6	105.0	1836.0	32.2	669.5	0.7	-12.1
0.3SZ42	239	5.56	455.3	39.0	19.5	54.5	8.7	105.0	1836.2	32.2	670.1	0.8	-10.4
0.3SZ46	243	5.45	450.4	39.0	19.5	54.5	8.2	102.5	1827.8	33.1	649.1	3.1	-5.4
0.3SZ48	245	5.39	462.9	39.0	19.5	54.5	9.6	108.8	1848.8	30.0	698.5	0.9	-10.0
0.3SZ50	247	5.34	472.3	39.0	19.5	54.5	10.6	115.0	1864.1	27.6	732.8	0.5	-9.9
0.3SZ52	249	5.28	460.1	39.0	19.5	54.5	8.8	107.5	1844.3	31.0	688.8	0.2	-12.1
0.3SZ58	255	5.21	456.8	39.0	19.5	54.5	8.9	105.8	1838.7	31.9	676.4	1.0	-10.9
0.3SZ60	257	5.20	466.7	39.0	19.5	54.5	9.9	110.7	1855.0	28.9	712.1	1.2	-10.6
0.3SZ62	259	5.20	472.3	39.0	19.5	54.5	10.4	115.0	1864.2	27.6	732.9	0.7	-11.3
0.3SZ64	261	5.19	444.2	39.0	19.5	54.5	7.9	99.4	1817.1	33.3	622.5	1.3	-11.1
0.4SZ0.5	263.85	5.18	704.4	73.0	39.0	54.5	22.7	249.2	2130.7	18.1	1348.3	0.9	-8.3
0.4SZ1.5	264.85	5.17	626.1	39.0	54.5	19.5	18.2	190.9	2062.5	21.1	1197.3	1.0	-10.5
0.4SZ3.5	266.85	5.17	460.9	39.0	19.5	54.5	9.2	107.8	1845.5	30.6	691.3	1.3	-9.0
0.4SZ5	268.35	5.16	434.0	19.5	54.5	8.8	7.4	94.7	1798.8	33.3	578.8	1.4	-8.1
0.4SZ7	270.35	5.15	454.7	39.0	19.5	54.5	8.6	104.7	1835.2	32.3	667.4	0.8	-11.9
0.4SZ11	274.35	5.14	487.4	39.0	54.5	19.5	11.9	127.0	1887.8	24.0	785.2	0.7	-11.1

0.4SZ13.0	276.35	5.13	490.5	39.0	54.5	19.5	12.9	128.1	1892.4	23.2	794.4	0.8	-11.4
0.4SZ15	278.35	5.12	507.8	39.0	54.5	19.5	14.6	138.6	1917.0	22.6	853.5	0.9	-11.4
0.4SZ17	280.35	5.11	508.9	39.0	54.5	19.5	14.0	139.5	1918.6	22.7	857.7	0.6	-11.4
0.4SZ19	282.35	5.10	518.4	39.0	54.5	19.5	15.4	142.9	1931.2	21.0	884.1	-0.1	-12.3
0.4SZ23	286.35	5.09	452.1	39.0	19.5	54.5	8.5	103.4	1830.7	32.7	656.3	1.1	-9.9
0.4SZ24.5	287.85	5.08	510.2	39.0	54.5	19.5	13.0	140.5	1921.6	23.8	866.9	1.3	-9.8
0.4SZ29.5	292.85	5.06	475.5	39.0	19.5	54.5	10.8	118.2	1869.2	26.8	744.3	1.2	-9.3
0.4SZ31.5	294.85	5.05	476.6	39.0	54.5	19.5	9.7	119.7	1871.5	28.3	751.6	0.8	-9.7
1SZ1.5	296.25	5.05	501.8	39.0	54.5	19.5	12.1	134.9	1910.1	24.2	838.5	1.1	-12.0
0.4SZ33.75	297.1	5.04	444.6	39.0	19.5	8.8	7.9	99.5	1817.7	33.3	624.1	1.6	-7.6
1SZ3.5	298.25	5.04	447.7	39.0	19.5	54.5	8.0	101.1	1823.1	33.3	637.5	0.9	-12.4
1SZ5.5	300.25	5.03	633.0	39.0	54.5	19.5	15.7	199.4	2068.1	21.3	1211.2	1.2	-10.1
1SZ9.5	304.25	5.01	620.3	97.5	73.0	54.5	21.0	194.3	2048.2	14.9	1139.5	0.0	-12.9
1SZ13.5	308.25	5.00	486.3	39.0	54.5	19.5	11.5	126.6	1886.2	24.6	782.5	0.9	-10.1
1SZ17.5	312.25	4.98	458.1	39.0	19.5	54.5	8.8	106.5	1841.0	31.5	681.6	1.2	-11.1
1SZ19.5	314.25	4.94	515.7	39.0	54.5	19.5	14.5	142.1	1927.8	21.9	877.9	0.6	-12.3
1SZ21.5	316.25	4.91	602.2	97.5	73.0	54.5	18.0	185.6	2031.8	16.4	1108.4	0.5	-11.8
1SZ23.5	318.25	4.88	464.0	39.0	19.5	54.5	8.9	109.4	1850.9	30.1	703.3	1.5	-9.4
1SZ25.5*	320.25	4.84	472.0	39.0	19.5	54.5	10.4	114.7	1863.7	27.7	731.8	1.2	-8.6
1SZ29.5	324.25	4.78	451.9	39.0	19.5	54.5	8.3	103.2	1830.4	32.8	655.4	1.6	-9.9
1SZ31.5	326.25	4.74	455.3	39.0	19.5	54.5	8.6	105.0	1836.2	32.2	670.1	1.0	-7.6
1SZ35	329.75	4.69	469.6	39.0	54.5	19.5	9.5	112.3	1859.9	28.3	723.2	1.1	-9.6
2SZ0.5	330.7	4.67	586.7	39.0	54.5	19.5	17.8	177.3	2016.3	19.0	1080.5	0.6	-11.9
2SZ2.5	332.7	4.64	465.9	39.0	19.5	54.5	9.4	110.3	1853.7	29.2	709.3	1.2	-9.7
2SZ4.5	334.7	4.60	467.0	39.0	19.5	54.5	9.5	110.9	1855.6	28.9	713.4	1.8	-9.8
2SZ8.5	338.7	4.54	474.7	39.0	54.5	19.5	10.5	117.4	1868.0	27.0	741.5	1.2	-9.7
2SZ12.5	342.7	4.49	451.6	39.0	19.5	54.5	8.3	103.1	1829.9	32.9	654.3	1.6	-10.8
2SZ14.5	344.7	4.47	450.2	39.0	19.5	54.5	8.1	102.4	1827.6	33.3	648.7	1.7	-10.4
2SZ16.5	346.7	4.45	760.3	97.5	73.0	54.5	18.3	445.3	2170.7	16.8	1436.3	-2.5	-13.3
2SZ20.5	350.7	4.43	645.6	97.5	73.0	39.0	17.7	208.0	2077.3	17.6	1220.6	0.3	-12.5
2SZ22.5	352.7	4.41	465.2	39.0	19.5	54.5	9.6	110.0	1852.7	29.3	706.9	0.7	-9.4
2SZ24.5	354.7	4.40	696.0	39.0	54.5	19.5	16.8	245.2	2127.9	21.6	1354.6	0.8	-8.6
2SZ26.5	356.7	4.39	528.1	54.5	39.0	19.5	12.0	146.6	1946.7	24.2	927.2	-0.3	-11.1
2SZ28.5	358.7	4.37	624.7	54.5	39.0	19.5	17.4	189.9	2061.1	20.5	1192.0	1.0	-10.7
2SZ30.5	360.7	4.36	638.6	73.0	39.0	54.5	14.6	201.7	2074.2	21.3	1225.7	0.8	-10.3
2SZ32.5	362.7	4.34	604.6	97.5	73.0	54.5	19.8	186.3	2032.1	15.0	1102.1	0.0	-11.3
2SZ34.5	364.7	4.33	674.8	39.0	54.5	19.5	12.5	224.6	2113.0	26.9	1331.4	-1.2	-12.0
2SZ36.5	366.7	4.32	568.0	54.5	39.0	19.5	15.8	167.2	1994.4	18.4	1026.6	-0.1	-12.4
2SZ38.5	368.7	4.30	592.3	39.0	54.5	19.5	10.9	170.0	2033.3	30.0	1144.5	0.9	-9.2
2SZ40.5	370.7	4.29	543.4	54.5	39.0	19.5	15.8	152.1	1963.7	19.1	957.4	-0.2	-11.7
2SZ42.5	372.7	4.28	574.8	73.0	54.5	39.0	18.4	170.6	2001.5	17.3	1039.9	0.4	-10.1
2SZ44.5	374.7	4.27	451.7	39.0	19.5	54.5	8.2	103.2	1830.1	33.0	654.8	0.7	-12.1
2SZ46.5	376.7	4.27	478.3	39.0	54.5	19.5	11.0	121.0	1873.6	26.0	754.4	0.4	-11.4
2SZ48.5	378.7	4.26	506.4	39.0	54.5	19.5	14.5	137.6	1915.0	22.6	848.4	0.4	-11.8
2SZ50.5	380.7	4.25	547.8	54.5	39.0	19.5	17.5	154.5	1968.6	18.7	967.2	-0.9	-12.3
2SZ52.5	382.7	4.25	486.8	39.0	54.5	19.5	11.4	126.8	1887.1	24.5	784.2	1.2	-10.2
2SZ54.5	384.7	4.24	466.6	39.0	19.5	54.5	9.7	110.7	1854.9	29.0	712.0	0.4	-9.7
3SZ36	422.2	4.06	538.7	54.5	39.0	19.5	15.1	149.7	1958.2	19.5	945.6	0.6	-11.3
3SZ38	424.2	4.04	866.4	97.5	73.0	39.0	19.5	754.0	2230.6	14.1	1558.4	1.0	-11.0

3SZ42	428.2	4.02	475.3	39.0	19.5	54.5	10.9	118.0	1868.9	26.8	743.5	0.5	-10.6
3SZ44	430.2	4.01	453.1	39.0	19.5	54.5	8.5	103.9	1832.5	32.6	660.8	0.7	-11.3
3SZ46	432.2	4.00	458.0	39.0	19.5	54.5	8.7	106.4	1840.7	31.7	681.0	1.4	-10.0
3SZ47.5	433.7	3.99	464.9	39.0	54.5	19.5	8.8	109.9	1852.5	30.0	706.9	1.7	-9.7
3SZ63	449.2	3.90	467.6	39.0	19.5	54.5	9.4	111.2	1856.7	28.7	715.9	1.0	-9.5
3SZ65	451.2	3.89	627.9	39.0	54.5	19.5	12.3	192.1	2067.8	25.1	1219.3	1.4	-6.5
3SZ69	455.2	3.87	578.5	73.0	54.5	39.0	17.4	172.6	2005.1	15.8	1042.2	0.2	-11.6
3SZ71	457.2	3.86	638.6	97.5	73.0	54.5	21.8	203.2	2064.9	13.9	1171.9	-0.1	-11.7
3SZ82	468.2	3.79	505.3	39.0	54.5	19.5	14.4	136.8	1913.5	22.7	844.7	1.9	-9.1
3SZ86.5	472.7	3.77	477.4	39.0	19.5	54.5	11.2	120.1	1872.2	26.3	751.0	-0.1	-8.3
3SZ88.5	474.7	3.75	478.6	39.0	54.5	19.5	10.3	121.6	1874.4	26.3	756.6	1.2	-8.3
3SZ90.5	476.7	3.74	548.2	54.5	39.0	19.5	17.1	154.8	1969.3	18.9	969.5	1.9	-9.0
3SZ92.5	478.7	3.73	476.0	39.0	19.5	54.5	10.9	118.7	1870.0	26.7	746.0	1.7	-11.7
3SZ94	480.2	3.72	503.5	39.0	54.5	19.5	13.8	135.7	1911.2	22.8	839.2	1.3	-9.7
3SZ105	491.2	3.66	490.7	39.0	54.5	19.5	12.5	128.2	1892.8	23.3	795.4	0.4	-11.5
3SZ107	493.2	3.65	523.6	39.0	54.5	19.5	16.1	144.6	1937.9	20.3	898.4	1.2	-11.5
3SZ109	495.2	3.64	516.1	39.0	54.5	19.5	15.3	142.1	1928.1	21.5	877.8	3.1	-6.8
3SZ111	497.2	3.63	556.8	54.5	39.0	19.5	17.4	160.1	1979.7	18.3	991.7	-0.3	-13.4
3SZ113.5	499.7	3.61	555.9	54.5	39.0	19.5	18.2	159.4	1978.4	18.2	988.3	0.0	-12.7
3SZ115.5	501.7	3.60	511.3	39.0	54.5	19.5	14.9	140.5	1921.7	22.4	864.8	2.6	-8.0
3SZ117.5	503.7	3.59	537.7	54.5	39.0	19.5	14.8	149.4	1957.0	19.6	943.0	2.7	-7.4
3SZ119.5	505.7	3.57	543.2	54.5	39.0	19.5	15.8	152.0	1963.6	19.2	957.2	2.5	-8.0
3SZ121.5	507.7	3.56	617.3	39.0	54.5	19.5	17.2	190.9	2051.2	19.5	1165.7	2.2	-9.6
3SZ123	509.2	3.55	510.8	39.0	54.5	19.5	14.4	140.4	1921.3	22.8	864.5	1.5	-10.4
4SZ0	526.8	3.40	693.5	39.0	54.5	19.5	16.9	244.2	2125.6	21.0	1347.3	1.4	-12.8
4SZ0.5	527.3	3.39	742.6	97.5	73.0	39.0	24.1	372.4	2158.4	17.4	1411.1	1.2	-8.0
4SZ1	527.8	3.39	808.4	97.5	73.0	54.5	25.8	592.6	2198.6	15.0	1490.0	1.7	-9.6
4SZ2	528.8	3.38	551.4	54.5	39.0	19.5	16.0	157.3	1974.2	19.4	982.3	-5.9	-16.5
4SZ3	529.8	3.37	967.2	147.5	127.5	97.5	44.7	962.8	2272.4	9.9	1600.8	0.2	-11.8
4SZ3.5	530.3	3.37	827.2	97.5	73.0	39.0	26.6	645.6	2209.3	14.8	1513.9	1.0	-10.7
4SZ4	530.8	3.36	709.2	97.5	73.0	54.5	19.1	264.6	2132.3	16.8	1346.2	1.2	-10.8
4SZ4.5	531.3	3.36	781.3	97.5	73.0	39.0	22.8	517.9	2183.8	16.7	1466.3	0.2	-11.2
4SZ5.5	532.3	3.35	603.5	39.0	54.5	19.5	17.7	181.2	2037.5	20.2	1136.1	0.9	-8.4
4SZ6	532.8	3.34	723.1	97.5	73.0	39.0	20.3	292.9	2145.6	18.4	1385.0	1.1	-9.2
4SZ6.5	533.3	3.34	487.6	54.5	39.0	19.5	9.6	127.3	1889.0	26.0	790.5	-2.0	-15.8
4SZ7.5	534.3	3.33	661.1	97.5	73.0	54.5	33.2	219.3	2085.8	14.2	1221.9	-0.4	-13.6
4SZ8	534.8	3.33	529.4	54.5	39.0	19.5	13.3	146.9	1947.0	21.3	922.7	-1.6	-15.5
4SZ8.5	535.3	3.32	546.0	73.0	39.0	54.5	18.6	153.3	1966.2	18.9	962.7	0.3	-11.5
4SZ9	535.8	3.32	552.5	73.0	39.0	54.5	18.8	157.3	1974.2	18.7	980.2	-0.9	-13.1
4SZ9.5	536.3	3.32	532.0	39.0	54.5	19.5	16.7	147.4	1948.9	19.6	923.2	-2.2	-13.8
4SZ10	536.8	3.31	552.8	54.5	39.0	19.5	16.1	158.1	1976.5	19.9	988.8	-1.3	-12.3
4SZ10.5	537.3	3.31	567.2	73.0	54.5	39.0	18.4	166.2	1992.6	18.0	1021.3	-3.5	-13.6
4SZ11	537.8	3.30	584.9	73.0	54.5	39.0	19.9	175.9	2011.9	15.9	1058.4	-1.6	-15.2
4SZ11.5	538.3	3.30	608.5	73.0	54.5	39.0	25.6	186.9	2036.7	15.5	1116.1	-5.3	-19.0
4SZ12.5	539.3	3.29	824.6	97.5	73.0	39.0	19.3	655.4	2211.2	17.4	1534.5	0.3	-9.5
4SZ13	539.8	3.29	679.2	73.0	54.5	39.0	21.5	233.1	2109.1	17.2	1292.9	0.7	-9.8
4SZ13.5	540.3	3.28	811.9	97.5	73.0	54.5	30.4	605.5	2201.2	15.4	1499.1	-0.6	-11.5
4SZ14.5	541.3	3.27	681.0	54.5	39.0	19.5	18.0	238.0	2112.4	18.7	1307.1	0.8	-12.5
4SZ16	542.8	3.26	878.8	97.5	73.0	54.5	35.5	774.8	2234.7	12.4	1551.8	-3.6	-19.4

4SZ16.5	543.3	3.26	525.3	54.5	39.0	19.5	14.9	145.3	1940.7	20.6	905.7	-2.4	-14.3
4SZ18.5	545.3	3.24	588.5	97.5	73.0	54.5	20.9	177.5	2014.8	15.2	1062.2	-3.4	-18.0
4SZ19.5	546.3	3.23	566.7	39.0	54.5	19.5	15.2	160.7	1998.3	22.2	1046.3	-0.8	-13.3
4SZ20	546.8	3.23	525.6	39.0	54.5	19.5	15.4	145.4	1941.1	20.8	907.3	-2.1	-15.5
4SZ20.5	547.3	3.22	529.4	39.0	54.5	19.5	15.1	146.7	1946.5	20.9	920.4	-2.6	-11.2
4SZ21	547.8	3.22	542.7	39.0	54.5	19.5	15.9	151.8	1963.7	20.1	960.0	-3.2	-13.0
4SZ21.5	548.3	3.21	545.9	39.0	54.5	19.5	17.0	153.7	1967.0	19.4	965.7	-2.2	-12.3
4SZ22.5	549.3	3.20	617.9	54.5	39.0	19.5	18.4	187.4	2052.7	19.2	1168.0	1.3	-9.1
4SZ24.5	551.3	3.19	510.4	39.0	54.5	19.5	13.4	140.4	1921.2	23.0	864.5	-1.9	-12.0
4SZ26.5	553.3	3.17	539.6	39.0	54.5	19.5	15.2	150.0	1960.1	20.6	952.9	0.6	-10.8
4SZ28	554.8	3.16	591.5	73.0	54.5	39.0	20.1	179.5	2018.9	15.7	1074.3	-3.2	-16.1
4SZ29	555.8	3.15	876.5	97.5	73.0	54.5	36.5	773.7	2234.5	13.3	1559.8	0.3	-13.3
4SZ29.5	556.3	3.15	623.4	97.5	73.0	54.5	35.2	194.6	2048.7	14.0	1135.1	0.5	-12.4
4SZ30.5	557.3	3.14	813.2	97.5	73.0	39.0	19.2	622.1	2204.6	17.2	1517.6	1.0	-11.8
4SZ31	557.8	3.13	848.6	97.5	73.0	39.0	27.2	710.7	2221.9	15.4	1547.4	-0.8	-12.7
4SZ31.5	558.3	3.13	586.5	73.0	54.5	39.0	20.6	175.4	2014.2	16.2	1065.5	0.8	-11.6
4SZ32	558.8	3.12	659.2	73.0	54.5	39.0	21.3	208.2	2092.2	17.8	1255.3	1.1	-11.8
4SZ32.5	559.3	3.12	932.5	147.5	127.5	97.5	44.5	889.3	2257.4	10.4	1577.1	0.9	-11.6
4SZ34	560.8	3.11	589.3	54.5	39.0	19.5	18.1	174.8	2020.4	18.7	1089.4	-5.6	-16.4
4SZ36.5	563.3	3.09	827.7	97.5	73.0	54.5	29.0	644.4	2209.1	14.5	1510.9	-0.6	-14.5
4SZ38.5	565.3	3.07	731.0	97.5	73.0	54.5	32.0	311.5	2145.9	15.2	1368.7	0.7	-15.7
4SZ40.5	567.3	3.05	555.9	54.5	39.0	19.5	15.2	160.3	1980.8	20.1	999.5	-0.2	-13.4
4SZ42	568.8	3.04	834.8	97.5	109.0	73.0	39.1	657.2	2211.6	13.0	1503.3	-0.4	-15.3
4SZ42.5	569.3	3.03	768.6	97.5	73.0	54.5	20.8	479.0	2176.6	17.3	1453.0	0.4	-12.7
4SZ44.5	571.3	3.02	557.2	54.5	39.0	19.5	17.6	160.5	1980.7	19.0	996.3	-1.2	-13.1
4SZ46.5	573.3	3.00	656.2	97.5	73.0	54.5	32.6	213.3	2080.5	13.8	1207.6	-0.2	-14.5
4SZ48.5	575.3	2.98	571.8	73.0	54.5	39.0	18.9	168.6	1997.3	16.6	1027.2	0.4	-12.9
4SZ50.5	577.3	2.97	722.0	97.5	73.0	54.5	30.7	286.9	2136.0	13.4	1333.1	0.8	-13.5
4SZ52.5	579.3	2.95	536.5	39.0	54.5	19.5	12.9	149.0	1958.2	24.2	955.8	1.0	-11.4
4SZ53.5	580.3	2.94	827.2	97.5	73.0	54.5	32.1	641.0	2208.4	13.8	1503.6	-0.3	-11.6
4SZ54	580.8	2.94	512.7	39.0	54.5	19.5	15.5	141.0	1923.4	22.0	868.0	0.8	-12.3
4SZ54.5	581.3	2.93	700.3	97.5	73.0	54.5	31.4	249.1	2119.8	14.0	1300.7	1.0	-13.1
4SZ55	581.8	2.93	594.7	39.0	54.5	19.5	16.7	179.2	2027.4	20.9	1112.8	0.0	-13.4
4SZ56	582.8	2.92	1253.1	2450.0			90.7	1452.5	2370.4	2.5	1212.2	0.2	-13.5
4SZ56.5	583.3	2.92	606.6	39.0	54.5	19.5	15.6	177.4	2045.4	23.4	1162.7	0.6	-11.3
4SZ57	583.8	2.91	757.0	97.5	73.0	54.5	19.4	436.1	2169.1	17.6	1437.0	0.0	-12.0
4SZ58	584.8	2.90	545.0	54.5	39.0	19.5	16.5	153.1	1965.7	19.2	962.2	-2.3	-15.2
4SZ58.5	585.3	2.90	605.8	97.5	73.0	54.5	26.7	186.2	2032.0	14.5	1099.3	-0.7	-14.6
4SZ60	586.8	2.89	529.1	54.5	39.0	19.5	16.0	146.5	1945.3	20.0	915.5	0.2	-14.7
4SZ62	588.8	2.87	583.3									-1.9	-15.2
4SZ62.5	589.3	2.86	556.1	54.5	39.0	19.5	17.8	159.6	1978.8	18.5	990.4	1.0	-12.9
4SZ63	589.8	2.86	560.7	39.0	54.5	19.5	14.2	154.8	1992.9	24.5	1037.7	1.9	-8.3
4SZ63.5	590.3	2.86	1185.8	2450.0	246.0	147.5	77.3	1348.2	2349.4	3.0	1319.1	0.7	-12.7
4SZ64	590.8	2.85	635.1	39.0	54.5	19.5	16.2	193.7	2073.3	22.9	1227.8	1.2	-12.5
4SZ64.5	591.3	2.85	810.1	97.5	73.0	39.0	19.9	611.6	2202.4	16.9	1511.1	1.6	-8.9
4SZ65	591.8	2.84	522.3	54.5	39.0	19.5	13.6	144.5	1937.5	22.1	901.1	0.9	-14.3
4SZ66.5	593.3	2.83	652.7	97.5	73.0	54.5	22.4	211.4	2078.9	14.2	1207.1	0.1	-13.0
4SZ67	593.8	2.83	509.5	39.0	54.5	19.5	12.9	140.2	1920.6	23.8	864.4	1.1	-12.9
4SZ67.5	594.3	2.82	518.6	39.0	54.5	19.5	14.2	143.2	1932.2	22.4	889.3	0.1	-13.5

4SZ68.5	595.3	2.81	641.4	54.5	39.0	19.5	16.5	197.2	2078.7	21.3	1236.7	0.8	-11.8
4SZ69.5	596.3	2.81	643.5	97.5	73.0	54.5	19.7	206.0	2072.0	15.1	1196.2	0.3	-11.9
4SZ70.5	597.3	2.80	490.9	39.0	54.5	19.5	12.5	128.3	1893.0	23.3	796.0	0.2	-12.7
4SZ72	598.8	2.78	544.5	54.5	39.0	19.5	14.6	153.3	1967.1	21.1	970.1	0.7	-12.4
4SZ74.5	601.3	2.76	536.1	54.5	39.0	19.5	14.8	148.9	1955.3	20.3	940.6	0.3	-12.6
4SZ76.5	603.3	2.75	939.6	97.5	109.0	73.0	32.4	917.0	2263.0	11.9	1609.9	1.3	-9.1
4SZ78.5	605.3	2.73	559.3	39.0	54.5	19.5	15.0	155.9	1989.4	22.7	1025.9	3.7	-10.1
4SZ79	605.8	2.72	533.8	54.5	39.0	19.5	17.0	147.9	1951.0	19.2	927.2	0.4	-13.0
4SZ79.5	606.3	2.72	658.3	97.5	73.0	54.5	18.3	220.4	2086.2	15.3	1229.5	0.4	-13.3
4SZ80.5	607.3	2.71	599.3	54.5	39.0	19.5	17.1	179.5	2032.9	20.2	1124.5	0.1	-15.0
4SZ81	607.8	2.71	736.7	97.5	73.0	54.5	22.7	337.0	2151.2	15.4	1382.8	1.2	-11.3
4SZ82	608.8	2.70	552.1	54.5	39.0	19.5	15.5	157.9	1975.9	20.1	988.1	-4.7	-19.4
4SZ82.5	609.3	2.69	502.8	39.0	54.5	19.5	12.7	135.5	1910.8	23.5	839.3	-1.9	-16.7
4SZ83	609.8	2.69	505.4	39.0	54.5	19.5	13.5	137.1	1914.0	22.9	846.5	-1.2	-15.1
4SZ84	610.8	2.68	577.2	54.5	39.0	19.5	16.1	170.4	2006.9	19.7	1060.3	-0.6	-14.4
4SZ84.5	611.3	2.68	825.9	97.5	73.0	39.0	26.7	642.0	2208.6	14.7	1511.0	0.7	-7.1
4SZ85	611.8	2.67	770.0	97.5	73.0	54.5	21.6	469.3	2174.7	15.3	1436.7	0.3	-12.6
4SZ85.5	612.3	2.67	508.8	39.0	54.5	19.5	14.4	139.4	1918.4	22.6	857.0	0.5	-11.8
4SZ86	612.8	2.67	519.3	39.0	54.5	19.5	15.5	143.2	1932.5	21.1	887.4	1.0	-12.2
4SZ86.5	613.3	2.66	737.8	97.5	73.0	54.5	19.5	354.0	2155.2	17.6	1404.6	0.9	-13.7
4SZ88	614.8	2.65	658.2	73.0	39.0	54.5	19.0	211.8	2090.9	18.2	1253.9	0.1	-13.0
4SZ90.5	617.3	2.63	826.4	97.5	73.0	54.5	22.7	651.4	2210.5	15.9	1523.7	1.0	-15.7
4SZ92.5	619.3	2.61	1284.3	54.5	39.0	19.5	18.6	238.4	2111.0	18.1	1301.2	-0.9	-13.2
4SZ94	620.8	2.60	508.3	39.0	54.5	19.5	13.2	139.3	1918.3	23.3	858.2	-1.8	-15.0
4SZ94.5	621.3	2.59	532.2	54.5	39.0	19.5	14.4	147.7	1950.7	21.4	931.6	0.4	-13.0
4SZ96	622.8	2.58	1263.2	2450.0			67.9	1520.2	2385.9	2.5	1247.6	1.8	-9.9
4SZ96.5	623.3	2.57	584.5	39.0	54.5	19.5	15.3	169.1	2019.3	22.2	1096.5	1.5	-11.1
4SZ97	623.8	2.56	1330.8	2450.0			206.2	1511.1	2382.0	2.2	1112.7	0.5	-8.2
4SZ98	624.8	2.54	816.4	97.5	73.0	39.0	19.4	622.2	2204.6	15.9	1510.1	1.8	-9.6
4SZ100.5	627.3	2.49	614.6	54.5	39.0	19.5	17.1	186.2	2049.8	20.1	1164.4	0.4	-11.2
4SZ102.5	629.3	2.45	605.5	97.5	73.0	54.5	28.4	185.3	2033.1	15.4	1106.7	1.3	-14.5
4SZ104.5	631.3	2.40	610.4	54.5	39.0	19.5	14.8	183.7	2047.6	22.7	1166.1	0.7	-10.9
4SZ106.5	633.3	2.36	593.6	97.5	73.0	54.5	19.4	180.5	2020.6	15.1	1075.3	0.9	-12.7
4SZ108.5	635.3	2.32	491.9	39.0	54.5	19.5	12.9	128.6	1894.5	23.1	799.0	0.8	-12.2
EZ Stratigraphic Section													
1 E.Z 3.8	3.8											-1.6	-11.7
1 E.Z 10	10											-7.8	-17.2
1 E.Z 24.5	24.5											-2.1	-11.8
1 E.Z 25.5	25.5											-5.8	-17.8
1 E. Z 27	27											-4.0	-16.1
1 E.Z 31.5	31.5											-1.2	-11.7
1 E.Z 35.5	35.5											-0.7	-11.7
1 E.Z 42	42											-4.4	-13.9
1 E.Z 44.75	44.75											-5.3	-16.3
1 E.Z 45	45											-2.9	-12.3
1 E.Z 46	46											-0.8	-11.8
1 EZ 52.2	52.2											-2.4	-11.2
2 E.Z 9	9											-1.2	-12.0
2 EZ 9.5	9.5											-6.8	-17.3

2 EZ 11.5	11.5	-4.2	-15.1
2 E.Z 14	14	-0.9	-12.1
2 E.Z 16.2	16.2	-3.0	-12.8
2 E.Z 18.5	18.5	-0.3	-11.7
2 EZ 22	22	-2.1	-11.8
2 EZ 60.7a	60.7	-1.2	-13.8
2 E.Z 63	63	0.6	-11.0
2 E. Z 67.5	67.5	0.4	-10.2
2 E.Z 68.5	68.5	0.5	-10.5
2 EZ 73	73	-0.2	-11.1
2 E.Z 88	88	0.0	-16.9
2 E.Z 89.4!	89.45	-0.1	-16.8
2 E.Z 92.9	92.9	-0.2	-11.7
2 EZ 115.5	115.5	-0.2	-11.6
3 E.Z 7	7	-4.2	-15.1
3 EZ 46	46	-3.8	-15.1
3 E.Z 63.5	63.5	-1.5	-13.3
3 EZ 69.2	69.2	-1.8	-15.2
3 E.Z 69.5	69.5	-1.6	-14.7
3 EZ 98	98	-1.3	-13.2
3 EZ 99	99	-1.4	-13.1
3 EZ 100	100	-1.4	-13.8
3 EZ 102	102	-1.7	-15.7
3 E.Z 108	108	0.8	-9.5
3 E.Z 111	111	-0.5	-13.4
3 E.Z 113.8	113.8	-0.9	-14.0
3 E.Z 116	116	-0.8	-14.5
3 E.Z 128	128	1.1	-9.5
3 EZ 131.3	131.3	2.2	-7.1
3 E.Z 133.!	133.5	-0.7	-14.4
3 EZ 135.3	135.3	-0.4	-12.4
3 E.Z 139	139	-0.6	-14.7
3 E.Z 139.!	139.9	-1.1	-14.1
3 E.Z 152	152	0.2	-11.4
3 EZ 154.5	154.5	0.5	-11.5
3 EZ 157	157	1.8	-10.3
3 E.Z 158	158	2.1	-9.7
3 E.Z 159	159	1.5	-11.1
3 EZ 161.5	161.5	1.4	-11.3
3 E.Z 167	167	-0.5	-12.5
3 E.Z 171	171	1.4	-10.1
3 EZ 173	173	2.9	-8.0
3 E.Z 174	174	1.3	-10.8
3 E.Z 180	180	0.4	-10.3
3 E.Z 183	183	1.8	-8.9
3 E.Z 186	186	0.9	-11.1
3 E.Z 187.!	187.5	0.0	-11.3
3 E.Z 191.!	191.5	0.1	-11.4
4 EZ 1	1	2.3	-8.8

4 EZ 4	4	-0.7	-12.6
4 EZ 6.4	6.4	0.7	-11.8
4 EZ 10.8	10.8	1.4	-10.9
4 EZ 11	11	-0.2	-13.3
4 EZ 12	12	-4.9	-15.9
4 EZ 17.7	17.7	-1.1	-13.8
4 EZ 22.7	22.7	-1.5	-14.3
4 EZ 25.3	25.3	0.0	-11.2
4 EZ 35.3	35.3	-0.3	-10.6
5 EZ 1.5	1.5	-0.6	-13.8
5 EZ 6.45	6.45	-1.6	-10.3
5 EZ 10	10	-0.2	-12.4
5 EZ 16.4	16.4	1.1	-11.0
5 EZ 27.75	27.75	1.2	-9.3
5 EZ 32	32	-3.0	-13.6
5 EZ 32	32	-1.1	-10.8
SEZ Stratigraphic Section			
1 SEZ 2	2.00	-0.1	-12.7
1 SEZ 9.2	9.20	-1.6	-11.8
1SEZ 24.25	24.25	-5.7	-15.3
2 SEZ 1.3	25.65	-1.7	-12.0
2 SEZ 7	31.35	-3.0	-12.8
3 SEZ 9	47.15	-7.0	-13.5
3 SEZ 29.5	67.65	-2.8	-13.4
3 SEZ 53	91.15	-0.7	-11.3
3 SEZ 58	96.15	0.0	-10.5
3 S.E.Z 71.5	109.65	-1.1	-11.5
4 SEZ 30.5	153.45	-1.2	-10.8
4 SEZ 30.5	153.45	-0.5	-10.6
4 SEZ 45.7	168.65	1.2	-11.0
5 SEZ 14.5	183.25	0.3	-11.0
5 SEZ 32.5	201.25	-1.9	-12.3
5 SEZ 42.6	211.35	0.2	-11.1
6 SEZ 8.5	223.05	-0.1	-11.1
6 SEZ 46.5	261.05	1.4	-8.1
6 SEZ 95	309.55	-1.4	-9.3
6 SEZ 96	310.55	-0.2	-11.1
7 S.E Z 7	318.75	0.8	-10.6
7 S.E Z 26.2	337.95	0.3	-10.4
8 S.EZ 23.8	373.95	1.2	-9.0
8 SEZ 28	378.15	0.7	-10.0
8 S.E.Z 32.5	382.65	1.7	-9.3

Table DR2: Means, standard deviations, and ANOVA statistics of mean grain size and $\delta^{18}O_c$ and $\delta^{13}C_c$ values from Zhada Basin.

	Interval A		**Interval B**		**Interval C**		**two sample *t* test A-B**			**two sample *t* test B-C**			**two sample *t* test A-C**		
SZ	**Mean**	**Std. Dev.**	**Mean**	**Std. Dev.**	**Mean**	**Std. Dev.**	**t stat**	**Deg. of freedom**	**p value**	**t stat**	**Deg. of freedom**	**p value**	**t stat**	**Deg. of freedom**	**p value**
Grain size	597.3	85.3	524.5	80.6	669.0	177.1	4.8	137	$3.0x10^{-6}$	-7.5	146	$5.8x10^{-12}$	3.4	158	$9.1x10^{-4}$
$\delta^{18}O$	-13.1	2.5	-10.4	1.6	-12.9	2.3	-9.5	103	$7.1x10^{-16}$	8.9	183	$6.4 x10^{-16}$	0.6	146	0.5
$\delta^{13}C$	-0.7	1.8	0.9	0.8	-0.2	1.7	-7.3	80	$1.7x10^{-10}$	6.0	159	$1.3x10^{-8}$	1.7	151	$9.8x10^{-2}$
R^2 ($\delta^{13}C$:$\delta^{18}O$)	0.37		0.50		0.48										
EZ															
$\delta^{18}O$	-13.4	2.2	-11.5	2.0			-3.9	77	$2.0x10^{-4}$						
$\delta^{13}C$	-1.9	2.1	0.2	1.5			-5.2	72	$1.9x10^{-6}$						
R^2 ($\delta^{13}C$:$\delta^{18}O$)	0.46		0.64												
SEZ															
$\delta^{18}O$	-13.1	1.2	-11.1	0.5	-9.7	1.0	-4.2	8	$3.1x10^{-3}$	-3.7	10	$4.3x10^{-3}$	6.0	12	$6.0x10^{-5}$
$\delta^{13}C$	-3.1	2.4	-0.4	0.9	0.6	1.0	-2.9	7	$2.4x10^{-2}$	-2.1	14	$5.9x10^{-2}$	-3.8	8	$5.6x10^{-3}$
R^2 ($\delta^{13}C$:$\delta^{18}O$)	0.50		0.33		0.68										

Table DR3. Lithofacies codes and interpretation

Lithofacies code	Description	Interpretation
Gcm	Conglomerate, clast-supported, poorly – moderately sorted, angular – sub-rounded, unstratified, poorly organized	Deposition by traction currents modified by shear forces, dispersive pressure or bouyancy
Gcmi	Conglomerate, clast-supported, poorly – moderately sorted, angular – sub-rounded, unstratified, imbricated	Deposition by traction currents
Gch	Conglomerate, clast-supported, poorly – moderately sorted, angular – sub-rounded, horizontally stratified	Deposition by traction currents in relative unconfined sheets
Gt	Gravel – pebble conglomerate, clast-supported, moderately – well sorted, rounded - sub-rounded, trough cross-stratified	Deposition by traction currents in sub-aqueous, migrating, three-dimensional gravel – pebble dunes
Gcf	Pebble conglomerate, clast-supported, moderately sorted, sub-angular – sub-rounded, planar or epsilon cross-stratified	Deposition by lateral or terminal accretion on bars
Gmm	Conglomerate, matrix-supported, poorly sorted, angular – sub-rounded, disorganized, unstratified	Deposition by cohesive mud- or sand-matrix debris flows
Gx	Conglomerate, matrix- or clast-supported, poorly sorted, angular - sub-rounded, disorganized, unstratified, with soft-sediment deformation	Deposition into a water saturated environment; post-depositional dewatering due to sediment compaction or due to bioturbation
St	Medium – very coarse sandstone with trough cross-stratification	Deposition by migrating three-dimensional sand dunes
Sp	Very fine – medium sandstone with planar cross-stratification	Deposition by migrating two-dimensional ripples
Sr	Very fine – medium sandstone with climbing ripple cross-stratification; occasionally interbedded with mudstone	Deposition under waning flow conditions; interbedding with mudstone indicates surging and waning flow conditions
Srw	Very fine – medium sandstone with symmetrical ripple laminations	Deposition under oscillatory current conditions
Sh	Very fine – medium sandstone with horizontal laminations	Deposition under unidirectional upper-flow regime conditions
Sm	Very fine – medium sandstone, unstratified	Deposition under conditions of extremely rapid sediment

		accumulation; alternatively bioturbation may have destroyed sedimentary structures
Sf	Very fine – fine sandstone with large planar foreset laminations	Deposition on the foresets of migrating sub-aerial dunes.
Sc	Very fine – very coarse sandstone with soft-sediment deformation, pre-existing sedimentary structures are usually obliterated	Deposition into a water saturated environment; post-depositional dewatering due to sediment compaction or due to bioturbation
Mr	Siltstone with climbing ripple cross-stratification	Deposition under waning flow conditions
Ml	Claystone – siltstone with horizontal laminations	Suspension settling in shallow standing water; laminations are often the result of layers of plant material
Mh	Claystone – siltstone with horizontal stratification	Suspension settling in deep water
Mm	Claystone – siltstone, unstratified	Post-depositional bioturbation
Mc	Claystone – siltstone with soft-sediment deformation	Post-depositional dewatering due to sediment compaction or bioturbation

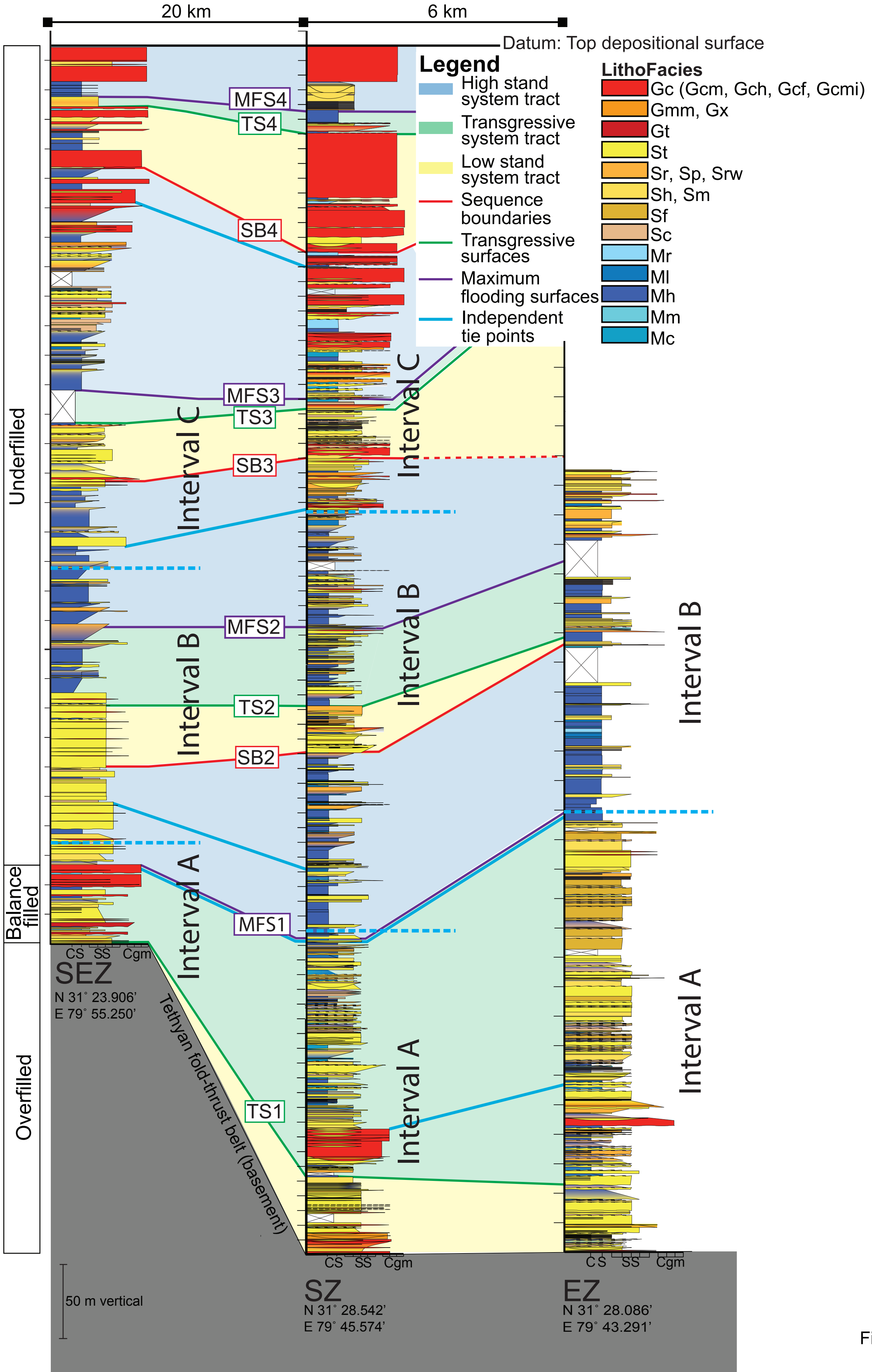
20 km
6 km
Datum: Top depositional surface
Legend
High stand system tract
Transgressive system tract
Low stand system tract
Sequence boundaries
Transgressive surfaces
Maximum flooding surfaces
Independent tie points
LithoFacies
Gc (Gcm, Gch, Gcf, Gcmi)
Gmm, Gx
Gt
St
Sr, Sp, Srw
Sh, Sm
Sf
Sc
Mr
Ml
Mh
Mm
Mc
Underfilled
Balance filled
Overfilled
MFS4
TS4
SB4
MFS3
TS3
SB3
MFS2
TS2
SB2
MFS1
TS1
Interval C
Interval B
Interval A
Tethyan fold-thrust belt (basement)
CS SS Cgm
SEZ
N 31° 23.906'
E 79° 55.250'
SZ
N 31° 28.542'
E 79° 45.574'
EZ
N 31° 28.086'
E 79° 43.291'
50 m vertical

Figure DR1

Figure DR2

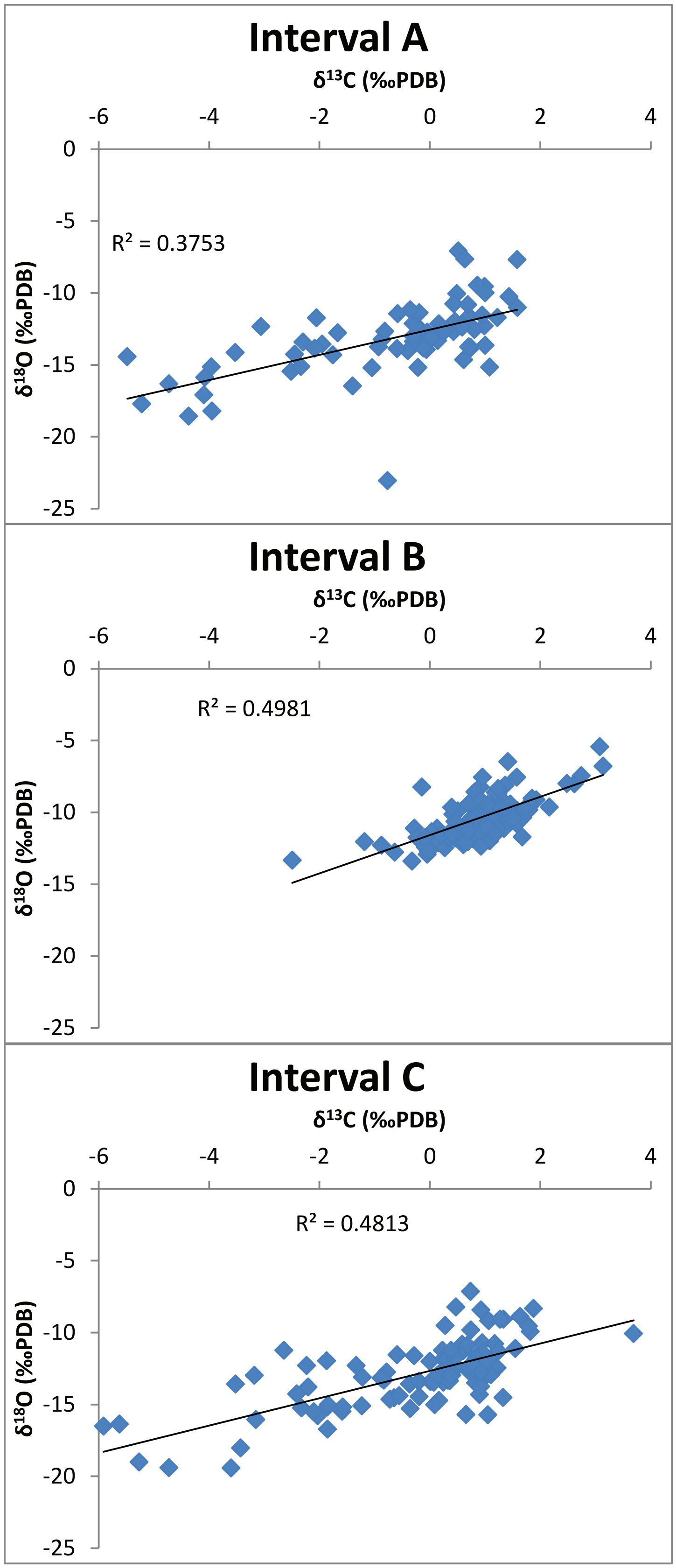

Interval A
δ13C (‰PDB)
-6
-4
-2
0
2
4
0
-5
-10
-15
-20
-25
δ18O (‰PDB)
R² = 0.3753
Interval B
δ13C (‰PDB)
-6
-4
-2
0
2
4
0
-5
-10
-15
-20
-25
δ18O (‰PDB)
R² = 0.4981
Interval C
δ13C (‰PDB)
-6
-4
-2
0
2
4
0
-5
-10
-15
-20
-25
δ18O (‰PDB)
R² = 0.4813

Figure DR3

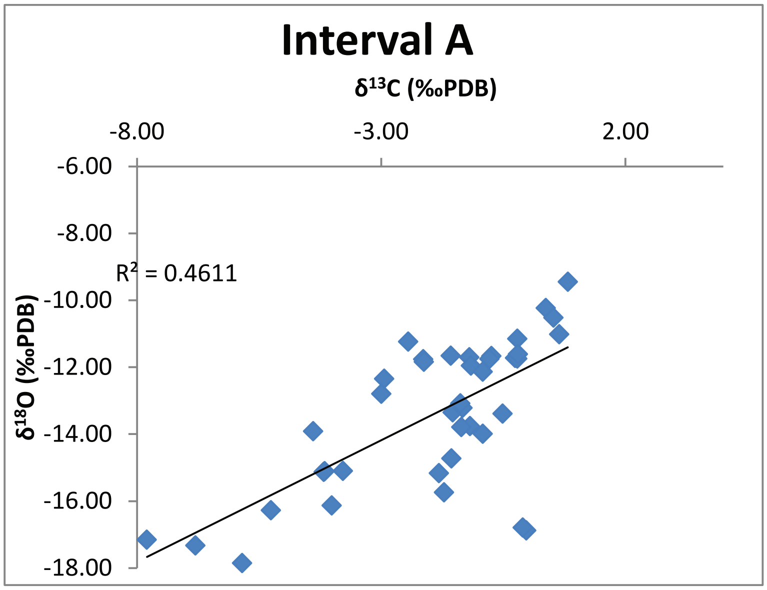

Interval A
δ13C (‰PDB)
-8.00
-3.00
2.00
-6.00
-8.00
-10.00
-12.00
-14.00
-16.00
-18.00
δ18O (‰PDB)
R² = 0.4611

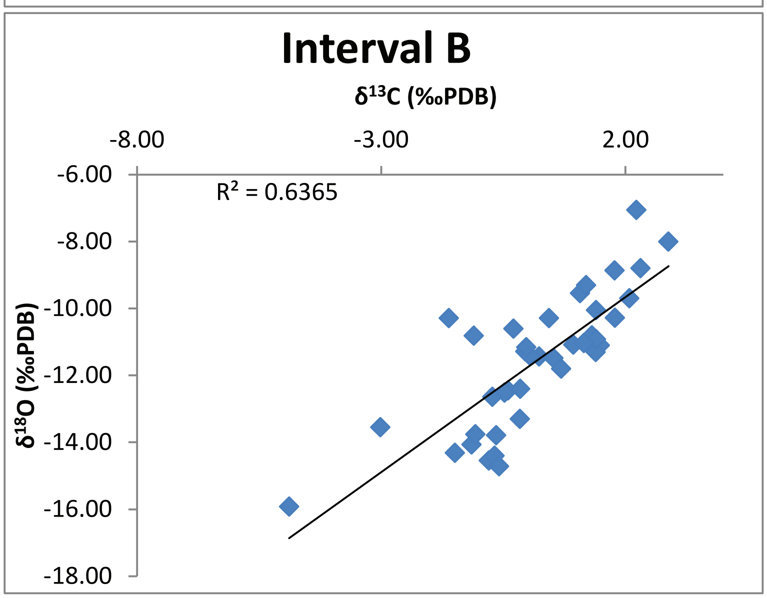

Interval B
δ13C (‰PDB)
-8.00
-3.00
2.00
-6.00
-8.00
-10.00
-12.00
-14.00
-16.00
-18.00
δ18O (‰PDB)
R² = 0.6365

Figure DR4

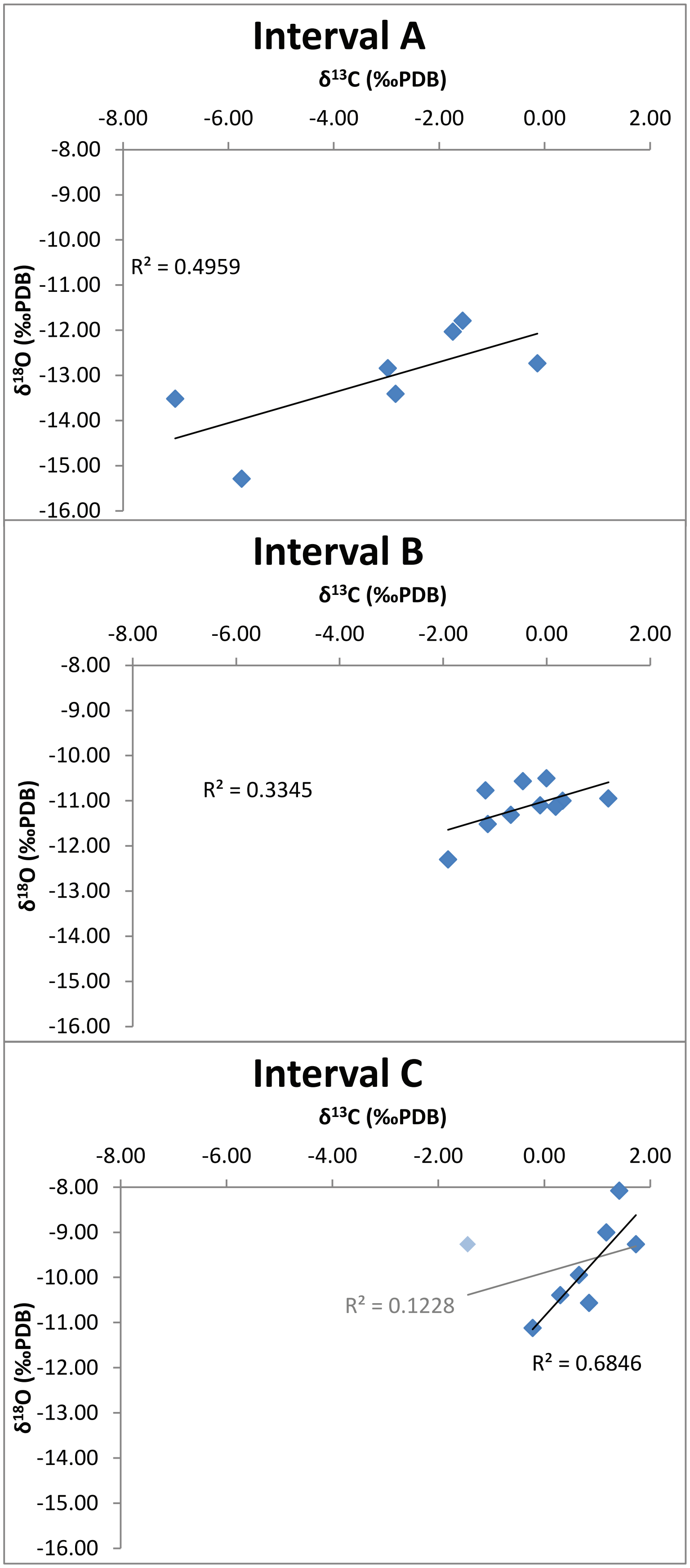
Interval A
δ13C (‰PDB)
δ18O (‰PDB)
-8.00
-6.00
-4.00
-2.00
0.00
2.00
-8.00
-9.00
-10.00
-11.00
-12.00
-13.00
-14.00
-15.00
-16.00
R² = 0.4959
Interval B
δ13C (‰PDB)
δ18O (‰PDB)
-8.00
-6.00
-4.00
-2.00
0.00
2.00
-8.00
-9.00
-10.00
-11.00
-12.00
-13.00
-14.00
-15.00
-16.00
R² = 0.3345
Interval C
δ13C (‰PDB)
δ18O (‰PDB)
-8.00
-6.00
-4.00
-2.00
0.00
2.00
-8.00
-9.00
-10.00
-11.00
-12.00
-13.00
-14.00
-15.00
-16.00
R² = 0.1228
R² = 0.6846